Applied Physics Letters

RESEARCH ARTICLE | JUNE 09 2023

Experimental verification of magnetic near-field channeling using a helical-shaped wire medium lens

Tiago A. Morgado ; Guilherme L. João ; Ricardo A. M. Pereira ; David E. Fernandes ; Sylvain Lannebère

Appl. Phys. Lett. 122, 231704 (2023)
https://doi.org/10.1063/5.0143807

Applied Physics Letters ARTICLE pubs.aip.org/aip/apl

Experimental verification of magnetic near-field channeling using a helical-shaped wire medium lens

Cite as: Appl. Phys. Lett. **122**, 231704 (2023); doi: 10.1063/5.0143807
Submitted: 26 January 2023 · Accepted: 23 May 2023 ·
Published Online: 9 June 2023

Tiago A. Morgado,[1,a] Guilherme L. João,[1] Ricardo A. M. Pereira,[2] David E. Fernandes,[3] and Sylvain Lannebère[1]

AFFILIATIONS

[1]Instituto de Telecomunicações and Department of Electrical Engineering, University of Coimbra, 3030-290 Coimbra, Portugal
[2]Instituto de Telecomunicações and Department of Electronics, Telecommunications and Informatics, University of Aveiro, 3810-193 Aveiro, Portugal
[3]Instituto de Telecomunicações, Avenida Rovisco Pais, 1, 1049-001 Lisboa, Portugal

[a]Author to whom correspondence should be addressed: tiago.morgado@co.it.pt

ABSTRACT

We experimentally verify that a magnetic uniaxial wire medium lens consisting of a racemic array of helical-shaped metallic wires may enable channeling the normal component of the magnetic field of near-field sources with resolution well below the diffraction limit over a broad bandwidth. It is experimentally demonstrated that the helical-shaped wire medium lens can be regarded as the magnetic counterpart of the usual wire medium lenses formed by straight metallic wires. The experimental results are validated with full-wave numerical simulations. We envision that the proposed metamaterial lens may have potential applications in magnetic resonance imaging, near-field wireless power transfer, and sensing.

The spatial resolution of conventional imaging devices is limited to about one half-wavelength, known as the diffraction limit. Manipulating the near field to overcome the diffraction limit is one of the most exciting applications of metamaterials. Various metamaterial-based subwavelength imaging systems have been proposed and discussed over the last two decades.[1–15] A particularly interesting mechanism is the one based on uniaxial arrays of parallel metallic wires that operate as almost perfect endoscopes and enable a pixel-by-pixel subwavelength channeling of the entire source-radiation spatial spectrum (the so-called "canalization regime.")[7–9,16–18] Yet, such wire medium lenses have an important polarization constraint as they only enable near-field imaging of transverse magnetic (TM) or *p*-polarized waves (magnetic field is parallel to the interface). For transverse electric (TE) or *s*-polarized waves (electric field is parallel to the interface), the wire medium lenses are fully transparent.

A solution to overcome the polarization sensitivity of the uniaxial wire medium lenses and fully restore the electric field radiated by a near-field source with arbitrary polarization was theoretically suggested[19] and experimentally demonstrated[20] some time ago. The proposed approach is based on the post-processing of three linearly independent measurements of the electric field using a metamaterial lens formed by an array of tilted metallic wires. However, such a solution only works for sources that radiate time-stationary fields.

A different possibility to achieve a channeling effect for TE polarized waves in wire medium lenses is by replacing the metallic wires with "perfectly magnetic conducting" (PMC) wires. Nonetheless, broadband PMC materials are mostly a theoretical idealization since they are not readily available in nature. Fortunately, it may be possible to exploit the unusual electromagnetic responses of artificial microstructured materials to engineer "magnetic wires." In Ref. 10, it was shown that arrays of "Swiss rolls"—periodic arrangements of cylinders comprising a thin conducting sheet wrapped around a central mandrel—provide a viable path to create PMC wires at MHz frequencies.

Sometime ago, we proposed an alternative way to imitate the response of PMC wires that can be implemented in the microwave regime and even possibly extended to higher frequency bands, based on a metamaterial consisting of a racemic array of helical-shaped metallic wires (designated as "magnetic uniaxial wire medium"[21]) [see Figs. 1(a) and 1(b)]. We theoretically and numerically demonstrated in Ref. 21 that such a metamaterial may be regarded to some extent as the magnetic analogue of the standard wire medium formed by straight metallic wires. In particular, it was shown that under a TE

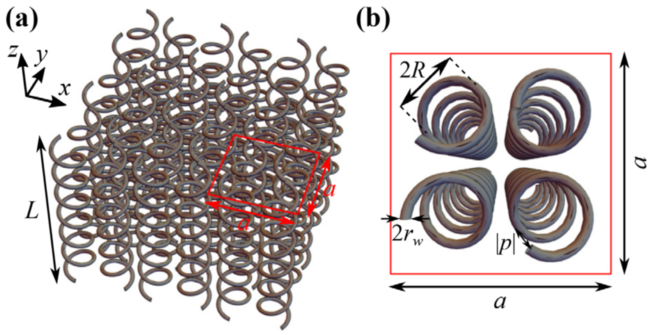

FIG. 1. (a) Geometry of the helical-shaped wire medium slab with thickness L: a racemic array of helical-shaped metallic wires periodic along the x and y directions (with lattice period a along both directions). (b) Unit cell of the metamaterial that includes two right-handed helices and two left-handed helices arranged in a checkerboard pattern.

excitation, the magnetic uniaxial wire medium supports a quasi-transverse electromagnetic (q-TEM) mode with phase velocity nearly independent of the transverse wave vector, similar to the mode supported by the standard wire medium for TM incident waves.[7–9] Moreover, we proved numerically that the magnetic uniaxial wire medium enables channeling the near field of TE polarized waves. The objective of this work is to experimentally confirm the findings of Ref. 21 and provide an experimental evidence of a magnetic near-field channeling effect at microwave frequencies.

The geometry of the considered metamaterial lens is illustrated in Fig. 1(a). It consists of a periodic array of helical-shaped metallic wires infinitely extended along the x and y directions. The unit cell is a square (with spatial period $a = 10$ mm) and contains four helical-shaped wires (specifically, two right-handed helices and two left-handed helices) arranged in a checkerboard pattern [see Fig. 1(b)]. The radius of the helical-shaped wires is $R = 0.2a$, the helix pitch is $|p| = 0.45a$, the radius of the wires is $r_w = 0.025a$, and the thickness of the lens along the z-direction is $L = 5a$. The free-space wavenumber and wavelength are respectively $k_0 = \omega/c$ and $\lambda_0 = 2\pi/k_0$.

Let us begin by discussing the transmission properties of the proposed metamaterial lens. To this end, we consider a scattering scenario where a TE plane wave propagating in the xoz plane ($k_y = 0$) with an electric field oriented along the y-direction illuminates the helical-shaped wire medium lens. It is worth noting that owing to the twofold rotational symmetry around the z-axis, the transmission properties are identical for a TE propagating in the yoz plane with the electric field oriented along the x-direction.

The transmission coefficient (T) of a metamaterial slab can be calculated using a nonlocal homogenization model that is reported in Ref. 21 and in the supplementary material. Figure 2(a) depicts the amplitude of T as a function of the transverse wave vector component k_x for several frequencies of operation. The solid curves are associated with the nonlocal homogenization model, whereas the star symbols were obtained with the full-wave electromagnetic simulator CST Studio Suite.[22] One can see that there is a good agreement between the two sets of results for both amplitude [Fig. 2(a)] and phase (see the supplementary material) of T. Notably, Fig. 2(a-i) predicts that for frequencies in the interval of 875–950 MHz, the transmission level exceeds unity ($|T| \geq 1$) over a significant range of the subwavelength (or evanescent) spatial spectrum ($1 < k_x c/\omega < 6$). This frequency interval is roughly centered around the Fabry–Pérot resonance ($k_z^{\text{q-TEM}} L = \pi$, with $k_z^{\text{q-TEM}}$ the z component of the wavevector of the q-TEM mode) of the lens, which occurs close to 900 MHz. On the other hand, even though the transmission level for the evanescent waves decreases substantially for frequencies below 875 MHz, the amplitude of T is still significantly different from 0 [see Fig. 2(a-ii)].

The subwavelength channeling effect with enhanced transmission ($|T| > 1$) reported in Fig. 2(a) is rooted in the excitation of two bulk modes: a q-TEM propagating mode that travels across the lens (along the z-direction) and a guided mode, which is responsible for the resonant enhancement (i.e., the peaks of $|T|$) and travels along the x-direction [see Fig. 2(b)].[21] In fact, the resonant transmission enhancement is an important qualitative difference compared to the TM canalization regime characteristic of the standard wire medium lenses formed by straight parallel metallic wires. The standard wire medium lenses are operated in a regime where there is no excitation of guided modes traveling parallel to the interfaces (i.e., perpendicular to the wires), such that the transmission coefficient does not exhibit a resonant behavior and $|T| \approx 1$ for both propagating and evanescent

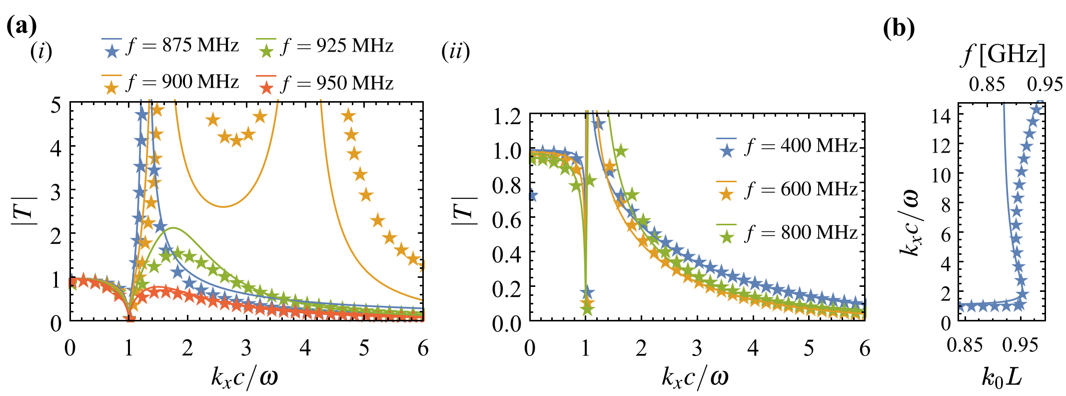

FIG. 2. (a) Amplitude of the transmission coefficient T as a function of the normalized transverse component of the wave vector k_x for different frequencies of operation. (b) Normalized propagation constant $k_x c/\omega$ of the low-frequency guided mode supported by the helical-shaped wire metamaterial as a function of the normalized frequency $k_0 L$. Solid lines: nonlocal homogenization results; star symbols: full-wave simulations.[22] The geometrical parameters in (a) and (b) are $a = 10$ mm, $R = 0.2a$, $r_w = 0.025a$, $|p| = 0.45a$, and $L = 5a$.

spatial harmonics.[23] On the other hand, the resonant transmission enhancement provided by the helical-shaped wire medium lens may be useful in practical applications, mainly because it may enable to compensate for the exponential decay of the evanescent waves outside of the lens. However, it also has some drawbacks. In particular, for a finite-width lens, the reflection of the guided modes at the edges of the lens may corrupt the quality of the imaging. Despite the qualitative difference between the two channeling mechanisms, the results of Fig. 2(a) clearly indicate that somewhat analogous to the standard wire medium lens that enables channeling the electric near-field details of TM polarized waves, the helical-shaped wire medium lens may enable the transport of the subwavelength details of TE polarized waves.

To experimentally verify the subwavelength imaging capabilities of the proposed metamaterial lens, we fabricated a prototype of the helical-shaped wire medium that consists of a finite-size periodic array of 36×36 helical-shaped steel wires (i.e., 18×18 square unit cells) [see Fig. 3(a)]. The helical-shaped wires [see Fig. 3(b)] are embedded in a Styrofoam block whose relative permittivity is close to unity around the considered microwave frequencies. To assess the magnetic near-field channeling potential of the metamaterial lens, we used a printed antenna formed by an array of four small magnetic loops parallel to the interface plane as the near-field source [see Fig. 3(c)]. The loops are disposed in the form of a square and placed at a subwavelength distance of each other so that the resolution capabilities of the lens along both x and y directions can be fully evaluated. In addition, the loops are fed by currents in phase (the phase of the current does not play an important role here) and are placed at a subwavelength distance (about 2.5 mm) from the input interface of the metamaterial lens. The z-component of the magnetic field (H_z) was measured 2.5 mm above the output interface of the lens using a near-field scanning system based on a robotic arm with a round shielded loop probe connected to a vector network analyzer (R&S ZVB20) [see Fig. 3(d)].

The measured H_z at the image plane and in the presence of the metamaterial lens is shown in Fig. 4(a) for different frequencies of operation in the range of $400 - 950$ MHz. In addition, the measured H_z at the source plane and in the absence of the metamaterial lens is represented in Fig. 4(b) for $f = 897.63$ MHz. It is clearly seen from Figs. 4(a) and 4(b) that, despite the subwavelength distance between the loops, the four magnetic loops are perfectly resolved at the image plane over a very broad frequency band (from 400 to 950 MHz). In contrast, the near-field radiation emitted by the loop array is completely imperceptible at the image plane when the metamaterial lens is removed [see Fig. 4(c)]. Thus, one can conclude that the imaging of the magnetic near field of the small loops is only possible because of the channeling effect provided by the helical-shaped wire medium lens.[21]

In the supplementary material, we also show the measured H_z at the image plane and in the presence of the metamaterial lens for a different separation between the loops ($\Delta \approx 83$ mm rather than $\Delta \approx 41.5$ mm). Such results are fully consistent with those of Fig. 4(a) and provide clear evidence that the channeling effect is not rooted in any special position of the near-field loops. It is worth noting that in both configurations ($\Delta \approx 41.5$ mm and $\Delta \approx 83$ mm), the loops are centered neither with the axis of the helices nor with the center of the unit cell.

A relevant aspect in the results shown in Fig. 4(a) is that the electromagnetic field distributions at the image plane are not fully symmetric along the x and y directions. In particular, the field intensity is not the same for all the four loops. The differences in the field intensities of the subwavelength loops (with perimeter in between $\lambda_0/10$ and $\lambda_0/25$) at the image plane are due to imperfections in the experimental setup. In particular, the distance between each loop and the lens input interface is not precisely the same. Due to the deeply subwavelength nature of the loops, their radiation properties (e.g., impedance) are highly sensitive to small disturbances. As a result, even minimal distance discrepancies can lead to significant differences in the field amplitude that reaches the input interface of the lens. These asymmetries are accurately reproduced by the lens at the image plane.

In order to confirm the experimental results of Fig. 4, the electromagnetic response of the same setup was simulated using the full-wave simulator.[22] Figures 5(a) and 5(b) depict the simulated z-component of the magnetic field, H_z, at the image plane and in the presence of the metamaterial lens [Fig. 5(a)], and at the source plane without the metamaterials lens [Fig. 5(b)]. The simulated fields are consistent with the experimental results of Figs. 4(a) and 4(b), and in particular, it can be seen from Fig. 5(a) that the four loops are clearly resolved at the image plane. Figure 5(c) provides a clear evidence of the magnetic near-field channeling effect performed by the helical-shaped wire

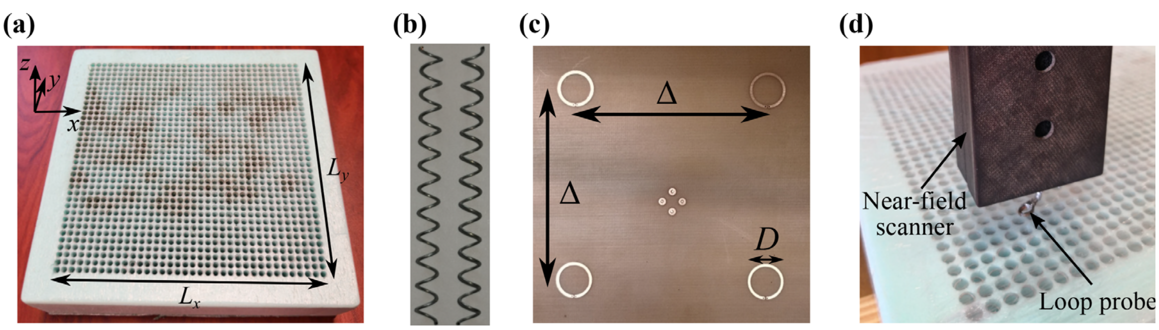

FIG. 3. (a) Photo of the prototype of the magnetic uniaxial wire medium lens formed by 36×36 helical-shaped steel wires with $R = 2$ mm, $|p| = 4.5$ mm, and $r_w = 0.25$ mm. The metamaterial lens has dimensions $L_x = L_y = 18a = 180$ mm and thickness along the z-direction $L = 5a = 50$ mm. (b) Photo of the two different metamaterial inclusions: a right-handed and a left-handed helical-shaped wire. (c) Photo of the excitation near-field antenna array formed by four small magnetic loops with $D \approx 9.5$ mm ($\lambda_0/80 \leq D \leq \lambda_0/30$ in the considered [400–950] MHz frequency band) and separated by a subwavelength distance $\Delta \approx 41.5$ mm ($\lambda_0/18 \leq \Delta \leq \lambda_0/8$ in the considered frequency range). (d) Photo of the experimental setup with the metamaterial lens and the near-field scanning system with a round shielded loop probe.

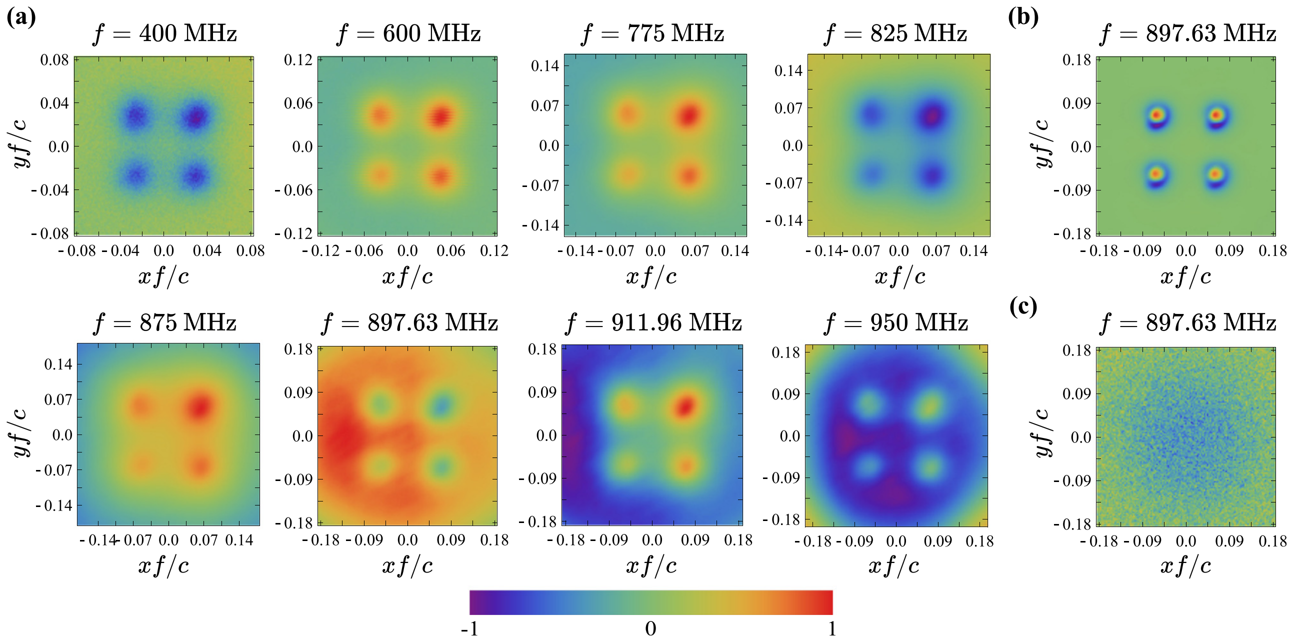

FIG. 4. Experimental time snapshots of the normalized z-component of the magnetic field for different frequencies; (a) at the image plane (about 2.5 mm above the output interface of the lens); (b) at the source plane (about 2.5 mm above the loop-antenna array) and in the absence of the metamaterial lens; and (c) at the image plane as in (a) but without the metamaterial lens.

metamaterial lens. As one can see, the radiation of the loops is clearly channeled by the metamaterial lens along the axial direction (z-direction) with negligible lateral spreading.

Notably, the magnetic field amplitude at the image plane in the presence of the metamaterial lens is different from zero on spatial regions significantly far from the position of the four loops. This property can be seen in the experimental results [Fig. 4(a)] for certain frequencies (e.g., $f = 897.63$ MHz, $f = 911.96$ MHz, and $f = 950$ MHz) as well as in the simulation results [Fig. 5(a)]. This happens because of the excitation of the guided modes traveling along the x and y directions of the metamaterial lens and due to the diffraction effects at the edges of the lens. In principle, microwave absorbers could be placed on the sides of the metamaterial lens to avoid these field interferences.

Due to the limited resolution of the metamaterial lens, the helical-shaped wire medium lens is unable to channel the finest details of the small magnetic loops to the image plane [see Figs. 4(a) and 5(a)]. For example, the magnetic field distribution of each loop is formed by a central maximum (ring) with another maximum with opposite phase surrounding it (annulus) [see Fig. 4(b)], but this structure is not perfectly reproduced at the image plane [see Figs. 4(a) and 5(a)]. The resolution of the helical-shaped wire medium lens is about twice the lattice period[21] (which corresponds to a resolution between $\lambda_0/40$ and $\lambda_0/16$ in the considered frequency range), whereas the distance between the two maxima of the magnetic field for each of the loops is much smaller than $2a$. For completeness, it is worth mentioning that an alternative version of the lens with two coaxial, interlaced, and non-connected helices with opposite handedness per unit cell

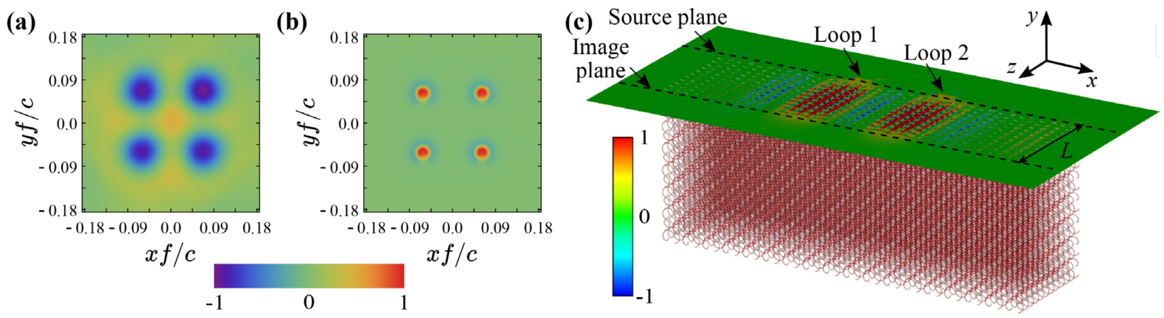

FIG. 5. Time snapshots of the normalized z-component of the magnetic field for $f = 897.63$ MHz, obtained using the full-wave electromagnetic simulator CST Studio Suite;[22] (a) at the image plane (about 5 mm from the output interface of the lens); (b) at the source plane (about 5 mm from the loop-antenna array) without the metamaterial lens. (c) At a xoz plane that cuts the metamaterial lens close to the middle of the lens and passes through the center of two loops. The remaining parameters of (a)–(c) are the same as in Fig. 4.

(i.e., with half spatial period) may potentially improve resolution by a factor of two.

In conclusion, we have experimentally verified that a magnetic wire medium lens based on a racemic array of helical-shaped metallic wires enables the channeling of the subwavelength details of the normal component of the magnetic field of near-field sources over a broad bandwidth. It was experimentally demonstrated that the magnetic wire medium lens effectively behaves as the magnetic analogue of the conventional wire medium lens formed by parallel straight metallic wires, enabling the sampling of the magnetic near-field distribution at the input interface of the lens and its transport to the output interface with little distortion. In principle, the design of this magnetic wire medium lens can be scaled to terahertz and infrared frequencies.[9] The reported magnetic channeling effect with subwavelength resolution provided by the proposed metamaterial lens may have important impact on several areas, such as in magnetic resonance imaging (MRI)[5,24] acting as a magnetic flux-guiding medium with super-resolution, in near-field wireless power transfer (NF-WPT)[25,26] by promoting a strong evanescent wave coupling and enhancing the power transfer efficiency, and in sensing of magnetic objects separated by subwavelength distances.[27]

See the supplementary material for the (i) nonlocal homogenization model that characterizes the electromagnetic response of the proposed helical-shaped wire metamaterial, (ii) the plane wave scattering problem based on the nonlocal homogenization approach, and (iii) further experimental results of the measured z-component of the magnetic field.

This work was funded by Instituto de Telecomunicações (IT) under project HelicalMETA—UIDB/50008/2020. T. A. Morgado acknowledges FCT for research financial support with reference CEECIND/04530/2017 under the CEEC Individual 2017 and IT-Coimbra for the contract as an assistant researcher with Reference CT/No. 004/2019-F00069. G. L. João acknowledges support by IT-Coimbra under a scientific initiation grant within the scope of the project HelicalMETA—UIDB/50008/2020. R. A. M. Pereira acknowledges support by FCT, POCH, and the co-financing of Fundo Social Europeu under the fellowship SFRH/BD/145024/2019. D. E. Fernandes acknowledges support by FCT, POCH, and the co-financing of Fundo Social Europeu under the fellowship SFRH/BPD/116525/2016 and by IT-Lisbon under the research contract with reference C-0042-2. S. Lannebère acknowledges financial support by IT-Coimbra under the research contract with Reference DL 57/2016/CP1353/CT0001.

AUTHOR DECLARATIONS

Conflict of Interest

The authors have no conflicts to disclose.

Author Contributions

Tiago André Morgado: Conceptualization (equal); Data curation (equal); Formal analysis (equal); Funding acquisition (equal); Investigation (equal); Methodology (equal); Supervision (equal); Validation (equal); Visualization (equal); Writing – original draft (equal). **Guilherme Luís João:** Data curation (equal); Investigation (equal); Writing – review & editing (supporting). **Ricardo A. M. Pereira:** Data curation (equal); Investigation (equal); Writing – review & editing (supporting). **David Fernandes:** Data curation (equal); Investigation (equal); Supervision (supporting); Writing – review & editing (equal). **Sylvain Lannebere:** Supervision (supporting); Writing – review & editing (equal).

DATA AVAILABILITY

The data that support the findings of this study are available from the corresponding author upon reasonable request.

REFERENCES

[1]J. B. Pendry, "Negative refraction makes a perfect lens," Phys. Rev. Lett. **85**, 3966–3969 (2000).
[2]N. Fang, H. Lee, C. Sun, and X. Zhang, "Sub-diffraction-limited optical imaging with a silver superlens," Science **308**, 534–537 (2005).
[3]A. Salandrino and N. Engheta, "Far-field subdiffraction optical microscopy using metamaterial crystals: Theory and simulations," Phys. Rev. B **74**, 075103 (2006).
[4]I. I. Smolyaninov, Y. J. Hung, and C. C. Davis, "Magnifying superlens in the visible frequency range," Science **315**, 1699–1701 (2007).
[5]M. J. Freire, R. Marques, and L. Jelinek, "Experimental demonstration of a $\mu = -1$ metamaterial lens for magnetic resonance imaging," Appl. Phys. Lett. **93**, 231108 (2008).
[6]A. Grbic, L. Jiang, and R. Merlin, "Near-field plates: Subdiffraction focusing with patterned surfaces," Science **320**, 511–513 (2008).
[7]P. A. Belov, Y. Hao, and S. Sudhakaran, "Subwavelength microwave imaging using an array of parallel conducting wires as a lens," Phys. Rev. B **73**, 033108 (2006).
[8]P. A. Belov, Y. Zhao, S. Tse, P. Ikonen, M. G. Silveirinha, C. R. Simovski, S. Tretyakov, Y. Hao, and C. Parini, "Transmission of images with subwavelength resolution to distances of several wavelengths in the microwave range," Phys. Rev. B **77**, 193108 (2008).
[9]M. G. Silveirinha, P. A. Belov, and C. R. Simovski, "Subwavelength imaging at infrared frequencies using an array of metallic nanorods," Phys. Rev. B **75**, 035108 (2007).
[10]M. C. K. Wiltshire, J. V. Hajnal, J. B. Pendry, D. J. Edwards, and C. J. Stevens, "Metamaterial endoscope for magnetic field transfer: Near field imaging with magnetic wires," Opt. Express **11**, 709–715 (2003).
[11]S. Maslovski, S. Tretyakov, and P. Alitalo, "Near-field enhancement and imaging in double planar polariton-resonant structures," J. Appl. Phys. **96**, 1293 (2004).
[12]M. G. Silveirinha, C. A. Fernandes, and J. R. Costa, "Superlens made of a metamaterial with extreme effective parameters," Phys. Rev. B **78**, 195121 (2008).
[13]S. Maslovski and S. Tretyakov, "Perfect lensing with phase-conjugating surfaces: Toward practical realization," New J. Phys. **14**, 035007 (2012).
[14]M. S. M. Mollaei and C. Simovski, "Dual-metasurface superlens: A comprehensive study," Phys. Rev. B **100**, 205426 (2019).
[15]M. Khorasaninejad, W. T. Chen, R. C. Devlin, J. Oh, A. Y. Zhu, and F. Capasso, "Metalenses at visible wavelengths: Diffraction-limited focusing and subwavelength resolution imaging," Science **352**, 1190–1194 (2016).
[16]G. Shvets, S. Trendafilov, J. B. Pendry, and A. Sarychev, "Guiding, focusing, and sensing on the subwavelength scale using metallic wire arrays," Phys. Rev. Lett. **99**, 053903 (2007).
[17]P. A. Belov, G. K. Palikaras1, Y. Zhao, A. Rahman, C. R. Simovski, Y. Hao, and C. Parini, "Experimental demonstration of multiwire endoscopes capable of manipulating near-fields with subwavelength resolution," Appl. Phys. Lett. **97**, 191905 (2010).
[18]H. Latioui and M. G. Silveirinha, "Near-field transport by a bent multi-wire endoscope," J. Appl. Phys. **120**, 063103 (2016).
[19]T. A. Morgado and M. G. Silveirinha, "Transport of an arbitrary near-field component with an array of tilted wires," New J. Phys. **11**, 083023 (2009).
[20]T. A. Morgado, J. S. Marcos, M. G. Silveirinha, and S. I. Maslovski, "Experimental verification of full reconstruction of the near-field with a metamaterial lens," Appl. Phys. Lett. **97**, 144102 (2010).

[21] T. A. Morgado, J. T. Costa, and M. G. Silveirinha, "Magnetic uniaxial wire medium," Phys. Rev. B **93**, 075102 (2016).
[22] SIMULIA – CST Studio Suite https://www.3ds.com/products-services/simulia/products/cst-studio-suite.
[23] P. A. Belov and M. G. Silveirinha, "Resolution of subwavelength transmission devices formed by a wire medium," Phys. Rev. E **73**, 056607 (2006).
[24] M. C. K. Wiltshire, J. B. Pendry, I. R. Young, D. J. Larkman, D. J. Gilderdale, and J. V. Hajnal, "Microstructured magnetic materials for RF flux guides in magnetic resonance imaging," Science **291**, 849–851 (2001).
[25] B. Wang, K. H. Teo, T. Nishino, W. Yerazunis, J. Barnwell, and J. Zhang, "Experiments on wireless power transfer with metamaterials," Appl. Phys. Lett. **98**, 254101 (2011).
[26] A. L. A. K. Ranaweera, T. P. Duong, and J.-W. Lee, "Experimental investigation of compact metamaterial for high efficiency mid-range wireless power transfer applications," J. Appl. Phys. **116**, 043914 (2014).
[27] M. G. Silveirinha, C. R. Medeiros, C. A. Fernandes, and J. R. Costa, "Resolving subwavelength objects with a crossed wire mesh superlens operated in back-scattering mode," New J. Phys. **13**, 053004 (2011).